

PCT/IL 2004/000613

08 JUL 2004

REC'D 29 JUL 2004

WIPO PCT

PA 1167373

THE UNITED STATES OF AMERICA

TO ALL TO WHOM THESE PRESENTS SHALL COME:

UNITED STATES DEPARTMENT OF COMMERCE

United States Patent and Trademark Office

May 06, 2004

THIS IS TO CERTIFY THAT ANNEXED HERETO IS A TRUE COPY FROM THE RECORDS OF THE UNITED STATES PATENT AND TRADEMARK OFFICE OF THOSE PAPERS OF THE BELOW IDENTIFIED PATENT APPLICATION THAT MET THE REQUIREMENTS TO BE GRANTED A FILING DATE UNDER 35 USC 111.

APPLICATION NUMBER: 60/485,731

FILING DATE: July 10, 2003

PRIORITY DOCUMENT
SUBMITTED OR TRANSMITTED IN
COMPLIANCE WITH
RULE 17.1(a) OR (b)

By Authority of the
COMMISSIONER OF PATENTS AND TRADEMARKS



P. SWAIN
Certifying Officer

BEST AVAILABLE COPY

PATENT APPLICATION SERIAL NO. _____

U.S. DEPARTMENT OF COMMERCE
PATENT AND TRADEMARK OFFICE
FEE RECORD SHEET

7/11/2003 HALLI1 00000036 60485731

1 FC:2005

80.00 OP

PTO-1556
(5/87)

**U.S. PATENT AND TRADEMARK OFFICE
PROVISIONAL APPLICATION FOR PATENT COVER SHEET**

This is a request for filing a PROVISIONAL APPLICATION FOR PATENT
under 37 C.F.R. §1.53(b)(2)

Atty. Docket: BANIN3

INVENTOR(S)/APPLICANT(S)			
LAST NAME	FIRST NAME	MI	RESIDENCE (CITY AND EITHER STATE OR FOREIGN COUNTRY)
BANIN	Uri		Jerusalem, Israel
EBENSTEIN	Yuval		Jerusalem, Israel
MOKARI	Taleb		Jerusalem, Israel
<input type="checkbox"/> Additional inventors are being named on separately numbered sheets attached hereto			
TITLE OF THE INVENTION (280 characters max)			
QUANTUM DOT FUNCTIONALIZED SCANNING PROBES FOR FLUORESCENCE ENERGY TRANSFER BASED MICROSCOPY			
CORRESPONDENCE ADDRESS			
Direct all correspondence to the address associated with Customer Number 001444, which is presently: BROWDY AND NEIMARK, P.L.L.C. 624 Ninth Street, N.W., Suite 300 Washington, D.C. 20001-5303			
ENCLOSED APPLICATION PARTS (check all that apply)			
<input checked="" type="checkbox"/> Specification	Number of Pages	14	<input checked="" type="checkbox"/> Applicant claims small entity status. See 37 C.F.R. §1.27
<input checked="" type="checkbox"/> Drawing(s)	Number of Sheets	5	<input type="checkbox"/> Other (specify) _____
METHOD OF PAYMENT (check one)			
<input checked="" type="checkbox"/> Credit Card Payment Form PTO-2038 is enclosed to cover the Provisional filing fee of <input type="checkbox"/> \$160 large entity <input checked="" type="checkbox"/> \$80 small entity			
<input checked="" type="checkbox"/> The Commissioner is hereby authorized to charge filing fees and credit Deposit Account Number 02-4035			

The invention was made by an agency of the United States Government or under a contract with an agency of the United States Government.

☒ No ☐ Yes, the name of the U.S. Government agency and the Government contract number are:

Respectfully submitted,

BROWDY AND NEIMARK, P.L.L.C.

By:

Sheridan Neimark
 Sheridan Neimark
 Registration No.: 20,520

Date: July 10, 2003

07/10/03
 15915 U.S. PTO

17613 U.S. PTO
 60/465731

07/10/03

Quantum dot functionalized scanning probes for fluorescence energy transfer based microscopy

*Y. Eberstein, T. Mokari, and U. Banin**

Institute of Chemistry the Farkas Center for Light Induced Processes, and the Center for Nanoscience and Nanotechnology, The Hebrew University of Jerusalem, Jerusalem 91904, Israel

banin@chem.ch.huji.ac.il

ABSTRACT

Semiconductor nanocrystals are used to functionalize an atomic force microscope (AFM) tip for fluorescence resonance energy transfer (FRET) microscopy. CdSe/ZnS nanocrystals are chemically bound to the surface of an AFM tip by three coating methods, utilizing organo-silane linker molecules. These methods were characterized on silicon and glass surfaces by AFM, scanning electron microscopy (SEM) and optical measurements. The unique photophysical properties of the quantum dots and their tunability via chemical synthesis are exploited to create light-emitting scanning probes with controlled emission color, using a single excitation source. These probes retain their sharpness for high-resolution topography acquisition. These properties are desirable for FRET schemes where the nanocrystals on the tip serve either as FRET donors or acceptors, interacting with chromophores on the scanned sample. This interaction provides a contrast mechanism for high resolution optical imaging in the near field. The potential of these coated tips for FRET based imaging is demonstrated by localized binding of acceptor dye molecules to the functionalized tips resulting in nearly complete FRET signals.

Introduction

High resolution optical imaging is an important tool in many fields of physical science, and especially in biology and medicine¹. Far field microscopy techniques are used extensively for imaging biological samples with diffraction limited resolution of $\sim 300\text{nm}$. Near field scanning optical microscopy (NSOM)^{2,3}, allows imaging with resolution below the optical diffraction limit by scanning sub-wavelength apertures in close proximity to the sample surface. The resolution of NSOM is typically on the order of 100nm with conventional tapered fiber probes⁴. It is difficult to improve the resolution of this technique to the molecular level due to the finite skin depth of the metal coating surrounding the fiber probe, and its low throughput and damage threshold⁵. This limitation can be overcome implementing apertureless-NSOM techniques^{6,7}. The contrast mechanism of these methods is based on detecting near field effects, locally induced by a sharp probe⁸. With the increasingly wide-spread and robust implementation of atomic force microscopy schemes, the apertureless-NSOM techniques also become more accessible.

One approach to enhance optical resolution is the exploitation of strongly distance dependant physical interactions such as FRET (fluorescence resonance energy transfer)^{9,10}. FRET is widely used in solution experiments^{11,12} and in single molecule spectroscopy¹³, to determine molecular scale distances in biological samples. The intensity of the FRET signal scales as the inverse sixth power of the distance between donor and acceptor molecules. The range of the FRET process can be estimated from R_0 , the distance where the interaction is at 50% efficiency, with typical values of $1\text{-}10\text{ nm}$. During the FRET process, energy is transferred non-radiatively through a dipole-dipole interaction from the excited donor chromophore, to the acceptor which fluoresces. Detection of the relative intensities of donor and acceptor fluorescence provides information regarding their relative distance and orientation¹⁴. This high sensitivity of FRET to molecular scale distances has been suggested as a contrast mechanism for high resolution optical imaging.

FRET based microscopy schemes are realized by the immobilization of donor or acceptor chromophores on the tip of a scanning probe microscope used to image the complimentary FRET

species on the substrate. As the functionalized tip approaches a chromophore on the substrate, Donor quenching and acceptor emission are induced by the FRET interaction, indicating the position of the chromophore with potential for molecular-scale resolution.

Several attempts to realize this imaging technique have been reported using pairs of dye molecules. Shubeita et al¹⁵ coated an NSOM tip with a polymer containing OM57 acceptor molecules while Vickery et al^{16,17} coated bare fiber probes with a dye containing lipid film or grew a dye containing polymer on silicon nitride AFM tips. The main technical challenges in these experiments are first to eliminate the cross-talk between donor and acceptor detection channels, caused by direct acceptor excitation and bleeding of the donor fluorescence signal to the acceptor channel. The photo-stability of the functionalized tips is an additional important issue for application of the method.

Semiconductor nanocrystals have several advantages over dye molecules as FRET donors. These advantages have also prompted their emerging use as novel biological markers in both in vitro^{18,19} and in-vivo applications^{20,21}. First, the nanocrystals may be tailored to provide exceptional spectral coverage through size and composition control with symmetric emission profiles, enabling optimization of donor-acceptor spectral overlap. Additionally, due to their continuous absorption band they may be excited efficiently at shorter wavelength regions where the acceptor dye molecule has minimal absorption cross section reducing direct acceptor excitation and hence donor-acceptor cross-talk. Finally, the nanocrystals are significantly more stable emitters compared to the conventional dye molecules and as mentioned above, this is a critical feature for a feasible FRET microscopy scheme. Recently, CdSe-ZnS quantum-dots were used as FRET donors in a model protein-protein binding assay demonstrating their advantages for FRET applications²².

In this paper, we describe a method to chemically bind CdSe/ZnS nanocrystals to silicon AFM tips for imaging purposes and especially FRET based microscopy. While writing this paper it has come to our attention that Shubeita et al have recently used semiconductor nanocrystals to coat NSOM fiber tips²³. In their case, tips were dipped in a polymer solution containing the nanocrystals to yield a 30-100nm thick layer of nanocrystal-stained polymer. Here, we employ a different approach, using organo-silane linker

molecules to attach the nanocrystals to conventional AFM tips. The functionalized tips manifest the optical characteristics of the bound nanocrystals while retaining the tip-sharpness for high resolution AFM imaging. We report distinct FRET interactions occurring on the tip apex after collection of acceptor dye molecules from the scanned surface. The high signal to noise ratio of this measurement demonstrates the potential of these probes for FRET imaging in the single molecule level.

Materials and methods

CdSe/ZnS nanocrystals and nanorods were prepared by the established methods of colloidal nanocrystal synthesis utilizing high temperature pyrolysis of organometallic precursors in coordinating solvents^{24,25,26,27}. Glass cover slips were sonicated in detergent solution for 15 minutes, thoroughly washed in distilled water and baked in an oven for 5 hours at 500°C yielding highly hydrophilic, optically clean glass. Silicon substrates and silicon AFM tips (mikromasch NSC11 and CSC12) were activated for 20 seconds in concentrated nitric acid to yield a clean, hydroxyl rich surface.

The surface of the substrates and the tips were silanized using aminopropyltriethoxysilane- APTES (Aldrich) or mercaptopropyltrimethoxysilane- MPTMS (Fluka), either in solution or in the gas phase. Gas phase silanization of the mercapto and amine terminated silanes was performed as follows: glass coverslips were placed on a Teflon holder inside a glass jar containing a few drops of organo-silane. The jar was sealed, heated to 70°C, and the coverslips were left to react overnight with the silane vapor. Silanization in solution was performed in a 2% (v/v) organo-silane ethanolic mixture where 5% high purity water was added. The mixture was left to hydrolyze for 5 minutes after which the glass coverslips were introduced into solution for an additional 2 minutes. In the case of MPTMS, rapid polymerization occurred upon addition of water to the mixture as could be seen by the formation of a white polymer-like solid.

After silanization, samples were washed with ethanol (Aldrich), dried with a flow of nitrogen and incubated for 3 to 6 hours in a 10^{-6} M solution of nanocrystals in toluene (Aldrich). After incubation, the samples were washed with toluene to remove unbound particles, dried with nitrogen flow and stored in

the dark under inert conditions until characterized. Dye stained λ -DNA (NEB- λ -DNA, molecular probes- BOBO-3) and dispersed dye molecules (Texas red, BODIPY TR-X-molecular probes & ATTO 590-sigma) were used as test-acceptor chromophores.

For HRSEM imaging of the tips, the cantilever was broken off the silicon chip and mounted directly on double sided carbon tape to minimize charging effects. Measurements were performed on a FEI-Sirion HRSEM with a field emission gun source using voltages of 2-10 kV.

AFM and optical measurements were performed using a system for correlated AFM and scanning fluorescence microscopy (see illustration in Figure 1)²⁸. Briefly, an AFM head (Digital Instruments- bioscope) is mounted on an inverted microscope (Zeiss- axiovert 100) equipped with a 100X, 1.4 NA oil immersion objective (Zeiss). The 458nm line of an argon ion laser (Melles griot- LAP 321) is focused to a tight spot on the sample surface, and excites the sample in an epi-illumination configuration. Fluorescence is collected by the same objective lens and directed either to a LN₂ cooled CCD spectograph (Princeton Instruments- LN-CCD1100, Acton-SP150) or to a dual-color avalanche photodiode (APD) arrangement (Perkin Elmer- spcm-14) for separate detection of donor and acceptor emission. For correlated topography and fluorescence measurements the AFM tip is positioned within the diffraction limited excitation spot and the sample is raster scanned by a separate piezo scanning stage (Nanonics- flatscan). This allows for simultaneous recording of the fluorescence and the topography of the sample, and at the same time provides an ideal setup for apertureless NSOM studies.

Results and Discussion

As a first step towards tip functionalization, an appropriate surface chemistry route to link nanocrystals to Si/SiO₂ surfaces was pursued using glass substrates as test-surfaces. Organo-silane molecules were reacted with the glass substrates providing a surface similar to that of oxidized silicon cantilevers, and then imaged with AFM to characterize the quality of the molecular coating. Two kinds of terminal groups, amine and thiol, were tested as potential linkers. These end groups, acting as coordinating groups in organic nanocrystal capping ligands, have a known affinity to the nanocrystal

surface. The linking is performed by incubating the silanized samples in nanocrystal solution. These samples were further characterized with AFM, SEM and optical spectroscopy measurements.

Silanized surfaces were characterized with AFM in contact mode. Figure 2 summarizes the AFM characterization of the different coating methods tested on glass coverslips. We used soft cantilevers (0.05 N/m) while applying minimal force. An attempt to use stiffer cantilevers resulted in severe damage to the organic layer while tapping mode AFM measurements resulted in anomalous height data and contrast reversal due to the force effect on the resonance frequency as we reported in an earlier study²⁹. The glass surface before silanization (Figure 2a) is clean and smooth with a mean roughness of 0.45 nm. The gas phase APTES treated cover slip shown in Fig. 2b exhibits a rough surface, with closely packed polymerized aggregates ranging between 30 to 90 nm in height. SEM imaging of similarly treated silicon revealed rodlike polymerization as seen in Fig. 2e. Amine-terminated silanes are indeed known to polymerize and the polymerization is somewhat reduced using solution phase linking. Figure 2c shows the surface after treatment with APTES in solution. Evenly distributed silane aggregates are seen, with heights ranging from 5 to 10 nm and average density of 2 aggregates per square microns. A considerably improved surface was obtained for the gas phase MPTMS treated glass. The roughness of the mercapto-silane functionalized surface is in the order of 0.3 nm and shows only occasional aggregation.

Substrates treated similarly to those discussed above were characterized with AFM after incubation in similar nanocrystal solutions (in this case we used 4 nm CdSe/ZnS dots). The bare glass surface showed only occasional large aggregates that did not wash away. Isolated small particles were not detected. It is important to note that it is very difficult to image unbound nanocrystals with contact mode AFM due to dragging of the particles by the tip. AFM parameters had to be carefully tuned to avoid dragging the particles on the substrate. In contrast to the bare glass, the silanized substrates show extensive binding of nanocrystals on all the surfaces. In these cases dragging was much less pronounced and we did not need to exercise special care in the AFM imaging to avoid it, indicating that the nanocrystals are bound to the substrates with relatively strong interaction. As may be expected from the images of the silanized

substrates, the MPTMS treated glass (figure 2h) exhibits the most uniform coverage of nanocrystals with no aggregation while the gas phase APTES treated glass (figure 2f) exhibits large nanocrystal aggregates. In figure 2h, a stronger lateral force was applied by the tip in the central 2micron region resulting in detaching of bound particles and dragging by the tip to the borders of the scanned area. Fluorescence measurements of the samples, excited by 514 nm, showed PL that is similar on all substrates, and closely matches the PL of the same nanocrystals in solution.

From the results of these silanization experiments, it is evident that the gas phase deposition of MPTMS is the most appropriate for tip coating. This method is easy to implement and yields high quality surface morphology. Minimum exposure to air and water should be exercised after silanization to avoid end group oxidation and contamination. The high affinity of the mercapto end group to the nanocrystal surface, results in high nanocrystal coverage after three hours of incubation in the nanocrystal solution. No effects on nanocrystal emission were observed. Using this coating method, AFM tips emitting various colors are easily prepared and may be tailored for specific applications.

Figure 3 shows HRSEM images of a functionalized AFM tip treated with MPTMS and coated with nanocrystals. For imaging purposes, this tip was functionalized with nanorods 4nm in diameter and 25 nm long. It is clear from figures 3a and 3b that the tip retains its general features and sharpness. Nanorods are identified on the tip apex but due to charging effects, it is difficult to resolve them. They can be clearly resolved covering the tip surface and most clearly on the tip cantilever which has the best contact to the conducting tape and therefore minimal charging problems (figures 3c and 3d respectively). Functionalization of the tip surface is therefore successfully implemented and nicely controlled where aggregation can be avoided. We note that the density of the nanocrystals coating the tip can be controlled by modifying the incubation time and concentration of the nanocrystal solution.

The emission spectrum from the same tip discussed above was measured with the fluorescence microscope setup and is traced in a dashed line in figure 4. The fluorescence is similar to that observed in solution for the same sample. To demonstrate the general applicability of this approach for functionalizing AFM tips with nanocrystals and nanorods, we performed similar linking experiments for

other nanocrystals. Fluorescence from three more coated tips is presented also in figure 4. The emission color from the tip is easily controlled by depositing nanocrystals of different sizes and in this case, emission spans the range from 556 nm for 3.5 nm CdSe/ZnS dots to 609 nm for 4x20 nm rods. The emission range of the functionalized tips could easily be extended to cover a broad range of wavelengths by connecting nanocrystals of other semiconductors from the wide variety of such samples that is presently available^{30,31,32,33}. Since the surface chemistry of II-VI, III-V and IV-VI semiconductor nanocrystals is similar, the same functionalization scheme could be used providing tips with emission from the blue to the NIR. Metal nanocrystals, for example gold, could be linked in similar fashion for microscopy schemes such as surface enhanced Raman.

An additional important issue for the functionalization process is that it should not hamper the performance of the AFM tip in topographic imaging. This was tested by imaging stretched DNA on glass with the tip emitting at 556nm. A cross section of the DNA image reveals a width at half maximum of 26 nm; similar to that achieved with an untreated tip and indicating that the tip remains sharp and capable of high resolution AFM imaging.

We next turn to attempts to observe FRET processes with the functionalized tips. For the FRET measurements, collected emission was split to two APD detectors using a 610nm dichroic mirror. With this setup, donor and acceptor fluorescence is detected independently [Weiss]. The sample presented here is a substrate with Atto-580 dye molecules. A dilute ethanolic solution of Atto-580 dye was spin cast on a clean glass coverslip resulting in separated single dye molecules. A tip functionalized with 570nm emitting nanocrystals was scanned over the excitation spot while collecting its fluorescence pixel by pixel to create the images in figure 5a and 5b. The right image, collected in the donor channel, represents mainly nanocrystal emission. It can be seen that the emitting area is n shaped with a size of approximately 1.5 x 1 microns and consisting of a bright right lobe and a weaker left region. The relative intensities are shown in the line section inset. Figure 5a, collected in the acceptor channel, represents acceptor dye emission together with the red nanocrystal emission tail. Here, the strongest signal (circled) correlates spatially to the weaker part in the donor image. This can be clearly seen if the two images are

superimposed as shown in figure 5c. Here, the green color represents donor emission while red represents acceptor emission, indicating that during scanning acceptor dye molecules have been collected at this region of the tip.

FRET between the nanocrystals and the dye molecules results in enhanced dye emission along with quenching of the nanocrystal emission. This observation was verified spectrally by taking localized spectra from different regions of the tip, and from isolated dye molecules on the surface. Figure 5d demonstrates the FRET interaction; the green, dashed spectrum, taken from the right tip region, is clearly dominated by the donor nanocrystal emission peak centered at 574 nm. The spectrum in solid red line was taken from the region with maximum emission in the acceptor channel and both donor and acceptor peaks are clearly resolved. The dotted black line is a spectrum of a single dye molecule peaking at 610 nm and recorded with higher excitation power due to the low direct excitation by the 458 nm laser line. The distribution of dye molecules on the substrate is 0-1 molecules per square micron, therefore only a few dye molecules could have been collected by the tip on the scanned area. This, together with the observed simultaneous enhancement and quenching of the acceptor and donor emission respectively, indicates that localized FRET interaction is observed on the tip.

Disengaging the tip from the surface, results in disappearance of the FRET signal, verifying that this interaction is indeed occurring on the tip surface. The inset in figure 5d shows another case where a functionalized tip collected dye molecules from the sample surface during scanning. The solid and dashed lines are FRET spectra of the tip while engaged and disengaged from the surface respectively.

The strong distance dependence of FRET interaction together with tip geometry serves to confine the active photonic volume for FRET to the tip apex. Clearly, the functionalized tips emit light with a micron scale area; yet, the FRET signal observed, is localized in an area equivalent to the excitation spot size with a diameter of approximately 400 nm. The fact that in this experiment all FRET signals come from the tip, which is scanned over the excitation spot, limits our resolution to the diffraction-limited spot size. It may very well be, as seen from SEM images of the tips, that for surface immobilized

acceptors, resolution could be significantly improved by over one order of magnitude. Such experiments are currently in progress.

Selective attachment of single nanocrystals to the tip apex is under investigation in our lab. Such tips can act as nanometric light sources for NSOM as demonstrated by Sandoghdar et al for a single dye molecule. For FRET based imaging, a large coated area can still result in a small active volume localized at the tip apex as shown in figure 5, based on the short-range of the FRET interaction.

The main drawback of this technique for imaging single molecules is their tendency to be collected by the functionalized tip. This was verified in solution experiments where we observed FRET signals from a mixed solution of texas-red dye molecules and nanocrystals, indicating spontaneous, non-specific binding of dye to the nanocrystal surface³⁴. Methods to overcome this problem are currently under investigation.

Conclusions

We developed a simple method for the functionalization of AFM tips with semiconductor nanocrystals. The resulting tips remain sharp, retaining the benefits of AFM imaging, and yet possess photophysical properties dictated by the attached nanocrystals. Emitting probes with various emission colors can be prepared and easily tailored for specific applications. These functionalized probes are especially attractive for imaging schemes based on FRET. The use of semiconductor nanocrystals as donors in such an imaging scheme resulted in high signal to noise ratio for FRET detection, enabling high collection efficiency and sensitivity to single molecule signal levels. The nature of the FRET interaction serves to confine the active photonic volume to the tip apex, thus enhancing potential imaging resolution with such probes.

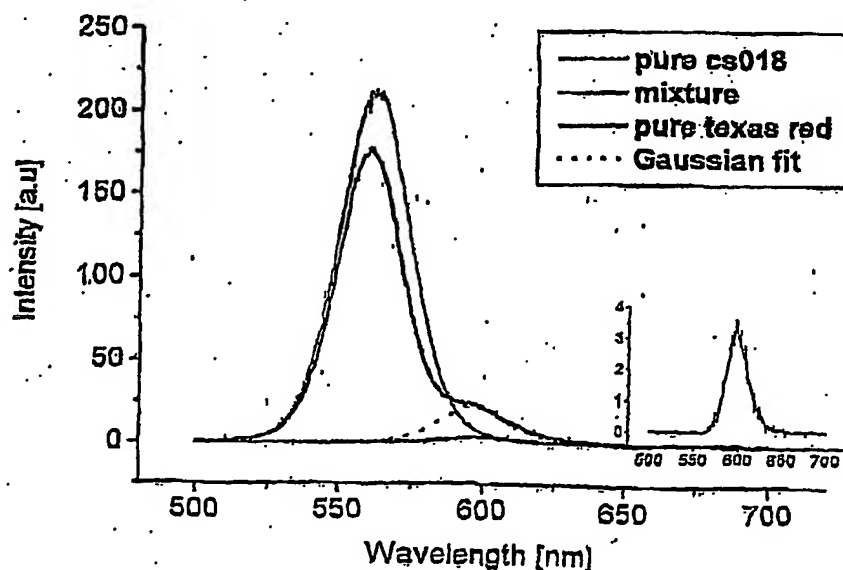
Acknowledgment

We thank Mila Palchan for performing the HRSEM imaging.

Supporting Information Available

Experimental details and results from solution FRET experiment demonstrating nonspecific, spontaneous binding of Texas red dye molecules to CdSe/ZnS nanocrystals.

Supporting information. Texas Red dye and CdSe/ZnS nanocrystals were dissolved in chloroform to prepare three solutions: a pure nanocrystal solution, a pure dye solution, and a mixture keeping the original concentrations of nanocrystals and dye. The PL of the three solutions was measured under 457nm excitation. The pure nanocrystal solution (green line) gave a distinct fluorescence signal peaking at 567 nm. The pure dye solution (red line), hardly fluoresces under this excitation wavelength and an enlarged representation is shown in the inset peaking at 604 nm, note that the fluorescence intensity is almost two orders of magnitudes weaker compared with the nanocrystal solution. The mixture fluorescence signal (black line) fits excellently to a Bi-Gaussian function with peaks closely corresponding to the nanocrystal and dye emission. Clearly, the nanocrystal emission quenches, and the dye emission is enhanced by close to one order of magnitude. Reabsorption of nanocrystal fluorescence by the dye molecules in the solution is minor in the concentrations used in this experiment, therefore we assume that spontaneous binding of dye molecules to the nanocrystal surface permits efficient FRET between the two chromophores. The slight blue-shift of the nanocrystal emission peak in the mixture supports this assumption.



References

- ¹ Herman, B. *Flourescence Microscopy, second edition*; Bios Scientific Publishers; 1998.
- ² Lewis, A.; Isaacson, M.; Harootmian, A. and Murray, A. *Ultramicroscopy* 1984,13, 227.
- ³ Betzig, E.; Trautman, J. K.; Harris, T. D.; Weiner, J. S.; Kostelak, R. L. *Science* 1991, 251, 1468.
- ⁴ Dunn, R.C. *Chem. Rev.* 1999, 99, 2891.
- ⁵ Novotny, L.; Pohl, D.; Hecht, B. *Opt. Lett.* 1995, 20, 970.
- ⁶ Zenhausem, F.; O'Boyle, M.P.; Wickramasinghe, H.K. *Appl. Phys. Lett.* 1994, 65,1623.
- ⁷ Furukawa, H.; Kawata, S. *Opt. Commun.* 1998, 148, 221.
- ⁸ Sanchez, E. J.; Novotny, L.; Xie, X. S. *Phys. Rev. Lett.* 1999, 82, 4014.
- ⁹ Kopelman, R.; Lewis, A.; Lieberman, K. *J. Lumin.*1990, 45, 298.
- ¹⁰ Sekatskii, S. K.; Letokhov, V. S. *JETP Lett.* 1996, 63, 319.
- ¹¹ Stryer, L.; Haugland, R.P. *Proc.Natl.Acad.Sci.USA*, 1967, 58, 719.
- ¹² Selvin, P.R. *Methods Enzymol.* 1995, 246, 300.
- ¹³ Ha, T.; Enderle, T.; Ogletree, D.F.; Chemla, D.S.; Selvin, P.R.; Weiss, S.; *Proc.Natl.Acad.Sci.USA*, 1996, 93, 6264.
- ¹⁴ Deniz, A. A.; Laurence, T. A.; Beligere, G. S.; Dahan, M.; Martin, A. B.; Chemla, D. S.; Daswon, P. E.; Schultz, P. G.; Weiss, S. *Proc.Natl.Acad.Sci.USA*. 2000, 97, 5179.
- ¹⁵ Shubeita, G. T.; Sekatskii, S. K.; Dietler, G.; Letokhov, V. S. *Appl.Phys.Lett.* 2002 , 80, 2625.
- ¹⁶ Vickery, S .A.; Dunn, R. S.; *Biophys.J.* 1999, 76, 1812.

-
- ¹⁷ Vickery, S. A.; Dunn, R. S. *J. Microsc.* 2001, 202, 408.
- ¹⁸ Chan, W. C. W.; Nie, S. *Science* 1998, 281, 2016.
- ¹⁹ Bruchez, M.; Moronne, M.; Gin, P.; Weiss, S.; Alivisatos, A.P. *Science* 1998, 281, 2013.
- ²⁰ Larson, D. R.; Zipfel, W. R.; Williams, R. M.; Clark, S. W.; Bruchez, M. P.; Wise, F. W.; Webb, W. W. *Science* 2003, 300, 1434.
- ²¹ Dubertret, B.; Skourides, P.; Norris, D.J.; Noireaux, V.; Brivanlou, A.H.; Libchaber, A. *Science* 2002, 298, 1759.
- ²² Willard, D. M.; Carillo, L.L.; Jung, J.; Van Orden, A. *Nano Lett.* 2001, 1, 469.
- ²³ Shubeita, G. T.; Sekatskii, S. K.; Dietler, G.; Potapova, I.; Mews, A.; Basché, T. *J. Microsc.* 2003, 210, 274.
- ²⁴ Murray, C. B.; Norris, D. J.; Bawendi, M. G. *J. Am. Chem. Soc.* 1993, 115, 8706.
- ²⁵ Hines, M. A.; Guyot-Sionnest, P. *J. Phys. Chem.* 1996, 100, 468.
- ²⁶ Talapin, D. V.; Rogach, A. L.; Kornowski, A.; Haase, M.; Weller, H. *Nano Lett.* 2001, 1, 207.
- ²⁷ Mokari, T.; Banin, U. *Chem. Mater.* 2003, Accepted.
- ²⁸ Ebenstein, Y.; Mokari, T.; Banin, U. *Appl. Phys. Lett.* 2002, 80, 4033.
- ²⁹ Ebenstein, Y.; Naftum, E.; Banin, U. *Nano Lett.* 2002, 2, 945.
- ³⁰ Murray, C. B.; Norris, D. J.; Bawendi, M. G. *J. Am. Chem. Soc.* 1993, 115, 8706.
- ³¹ Weller, H.; Koch, U.; Gutiérrez, M.; Henglein, A. *Berichte der Bunsengesellschaft Physical Chemistry* 1984, 88, 649.

³² Bowen Katari, J. E. B.; Colvin, V. L.; Alivisatos, A. P. *J. Phys. Chem.* 1994, 98, 4109.

³³ Cao, Y. W.; Banin, U. *J. Am. Chem. Soc.* 2000, 122, 9692.

³⁴ See supporting information for details

Figure Captions

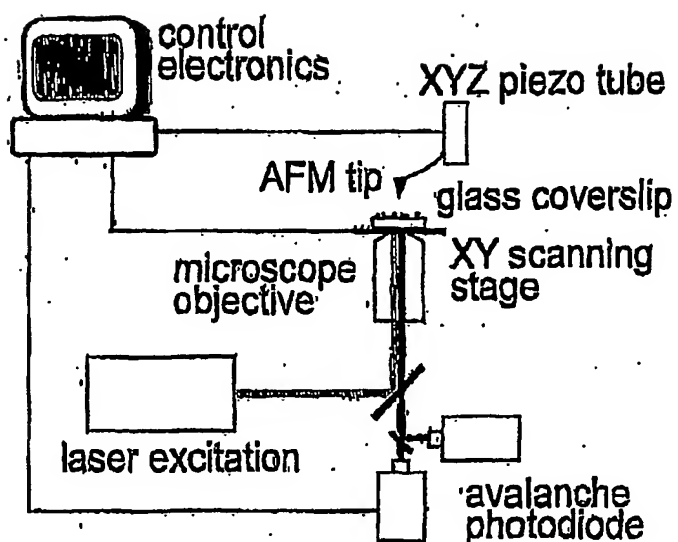


Figure 1. Schematic representation of the experimental system for correlated AFM and optical measurements.

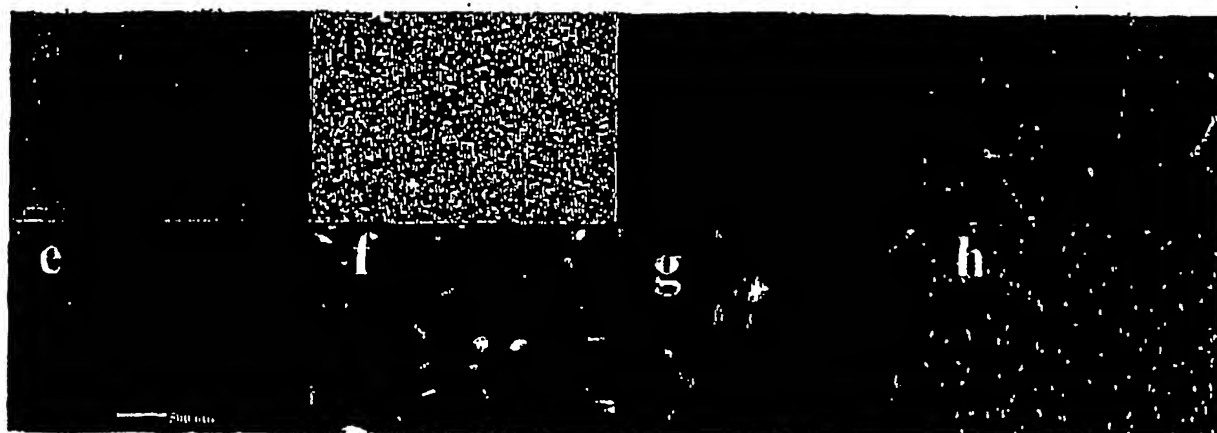


Figure 2. AFM images of glass substrates after the various treatments tested: Clean glass-a; glass functionalized with APTES in the gas phase, before- b, and after-f incubation in nanocrystal solution; glass functionalized with APTES in solution, before- c, and after-g incubation in nanocrystal solution; glass functionalized with MPTMS in the gas phase, before- d, and after-h incubation in nanocrystal solution; SEM image of a gas phase APTES functionalized silicon chip- e.

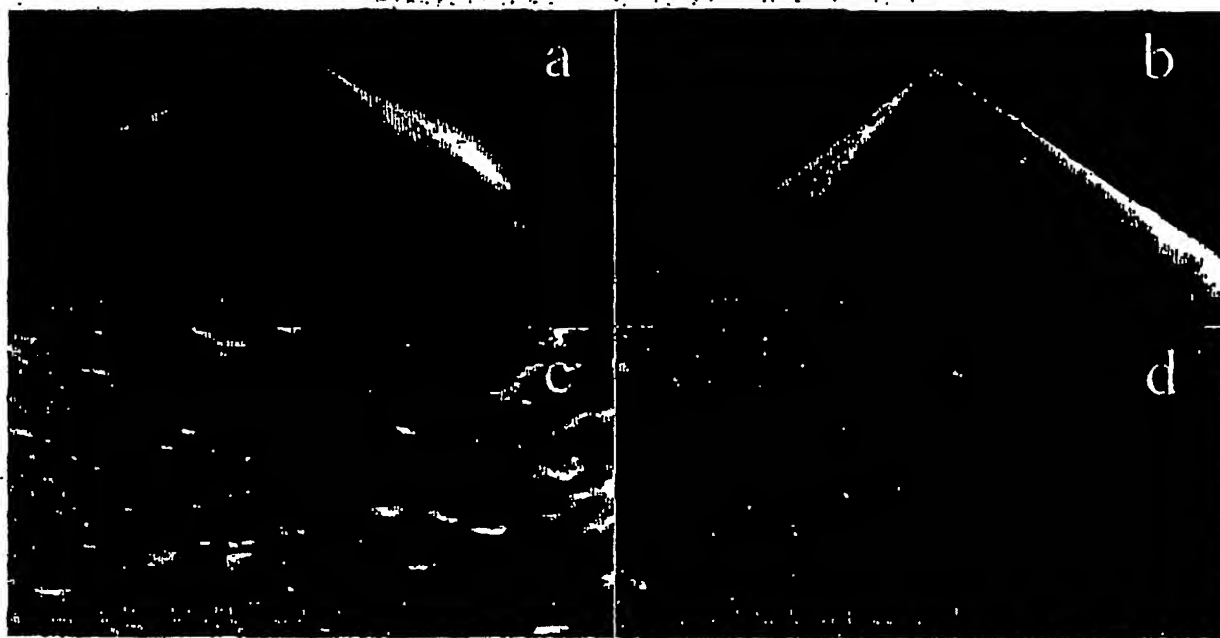


Figure 3. SEM images of a MPTMS–nanorod functionalized tip: a- general view; b,c,d- close up on the tip apex, tip surface and cantilever respectively. Due to charging effects, nanorods are resolved more clearly as imaging is done closer to the conducting substrate.

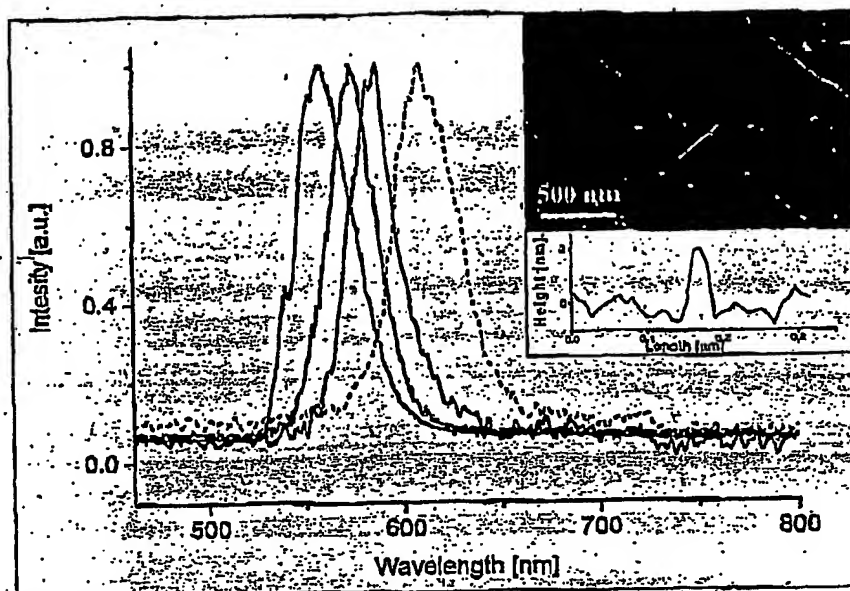


Figure 4. Emission spectra of four functionalized tips ranging from 556 to 609 nm, including the tip imaged in fig. 3. (dashed). Inset- AFM image and line section of stretched DNA on glass acquired by the tip emitting at 556 nm.

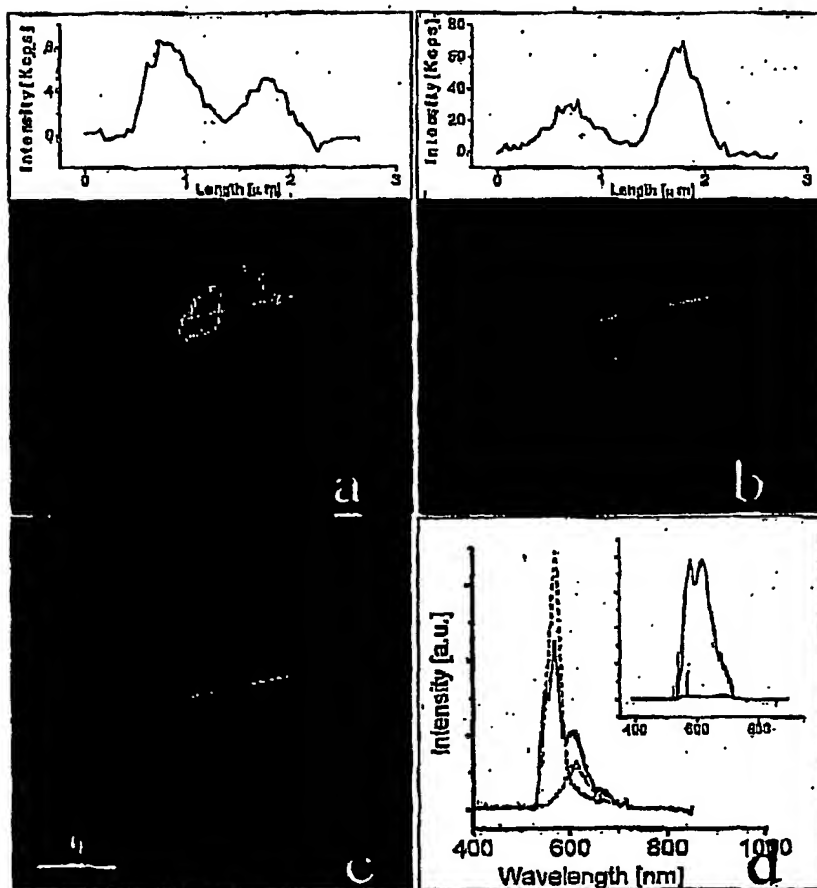


Figure 5. Demonstration of local FRET between nanocrystals on the functionalized tip and dye molecules collected by the tip while scanning the surface: **a-** optical image acquired in the acceptor channel, and its line section showing dominant signal intensity on the left region; **b-** optical image acquired in the donor channel and its line section showing dominant signal intensity on the right region; **c-** super imposed image representing spatially localized donor (green) and acceptor (red) emission from the tip; **d-** spectra taken from: a single dye molecule on the surface emitting at 610 nm (black, dotted line), the central tip region showing pure nanocrystal emission at 574 nm (green, dashed line), and the left tip region where both peaks are resolved, demonstrating the FRET interaction (red, solid line);

**This Page is Inserted by IFW Indexing and Scanning
Operations and is not part of the Official Record**

BEST AVAILABLE IMAGES

Defective images within this document are accurate representations of the original documents submitted by the applicant.

Defects in the images include but are not limited to the items checked:

- ☐ BLACK BORDERS
- ☐ IMAGE CUT OFF AT TOP, BOTTOM OR SIDES
- ☒ FADED TEXT OR DRAWING
- ☒ BLURRED OR ILLEGIBLE TEXT OR DRAWING
- ☐ SKEWED/SLANTED IMAGES
- ☐ COLOR OR BLACK AND WHITE PHOTOGRAPHS
- ☐ GRAY SCALE DOCUMENTS
- ☐ LINES OR MARKS ON ORIGINAL DOCUMENT
- ☒ REFERENCE(S) OR EXHIBIT(S) SUBMITTED ARE POOR QUALITY
- ☐ OTHER: _____

IMAGES ARE BEST AVAILABLE COPY.

As rescanning these documents will not correct the image problems checked, please do not report these problems to the IFW Image Problem Mailbox.